Jurnal Kejuruteraan 35(6) 2023: 1419-1426
https://doi.org/10.17576/jkukm-2023-35(6)-14

Cavitation in Internal Flows of Liquid Jet Through a Throat

Ahmad H. A. Hamid, Azmi A. Matali, Z. A. Ghaffar & S. Kasolang*

School of Mechanical Engineering, College of Engineering, Universiti Teknologi MARA, 40450 Shah Alam, Selangor, Malaysia

**Corresponding author: zulkiflighaffar@gmail.com*

Received 5 April 2022, Received in revised form 9 May 2023
Accepted 9 June 2023, Available online 30 November 2023

ABSTRACT

The interaction of a liquid with the surrounding air produces unstable waves that disintegrate the liquid into droplets, which is known as liquid atomization. The common internal flow of a liquid atomization nozzle experiences a single-phase flow but might turn into a multiphase flow with the existence of cavitation. Cavitation in internal flow has gotten a lot of attention because of the positive and negative consequences it can have depending on the application. One such advantageous result is that cavitation has been used to promote the atomization of liquid jets by causing gas bubbles in the atmosphere to collapse. Most of the past research on cavitation has focused on the exit orifice's constant cross-section area. The current study investigates the effect of throat location and geometry on cavitation characteristics. Filtered water was used as the simulation fluid. The high-speed shadowgraph technique was applied to record the images of the internal flow patterns. The placement of the throat was discovered to have a substantial impact on the status of the cavitation. Cavitation began at the inlet of the throat when the throat was placed at the uppermost part of the exit orifice. However, when the throat is placed in the middle of the exit orifice, the cavitation begins at the end of the throat. Four cavitation regimes were identified, namely developing, mixed, super and sudden expansion cavitation. Furthermore, it was found that the discharge coefficient depends on the cavitation's state and length, except when the cavitation is in the supercavitation regime.

Keywords: Cavitation; atomization; discharge coefficient; cavitation length; shadowgraph

INTRODUCTION

Liquid jets issued from an orifice are fascinating due to their many practical applications, such as spray drying (Ali Othman & Fahmi Mohd Razali 2019), surface cooling (Etminan & Harun 2021) and fuel injection in the combustion chamber (Wei et al. 2023). The liquid interacts with the surrounding air to produce unstable waves, which disintegrate into fragments and contract into ligaments. These ligaments then break down into droplets (Lefebvre & McDonell 2017). This phenomenon is known as liquid jet atomization. The breakup mechanism and atomization will determine the characteristics of the resulting spray.

The flow of this type of nozzle is usually single phase. However, the flow becomes multi-phase when cavitation occurs within the nozzle (Abderrezzak & Huang, 2016; Daikoku & Furudate, 2003; Li et al. 2018; Lü et al. 2015; Qiu et al. 2022; Sher et al. 2008; Shervani-Tabar et al. 2012). This phenomenon occurs when the liquid pressure in the system falls below the vapor pressure. The liquid will flash into vapor and form vapor bubbles, also known as cavitation bubbles (Wang et al. 2018). Its collapse within the liquid follows the rapid formation of these bubbles. Two types of bubble nucleation may occur in the cavitation processes, i.e., homogeneous nucleation, which occurs within the liquid, and heterogeneous nucleation, which initiates from boundaries such as the wall. The cavitation in a liquid jet is different from the effervescent atomizer in that the pressure of cavitation gas bubbles is lower than the liquid pressure.

When cavitation occurs, vapor bubbles violently implode when the jet flow leaves the orifice into the surrounding ambient, causing the enhancement of liquid jet breakup. Abderrezzak et al. (2016) reported that the liquid jet breakup (droplet formation and spray angle) is dominated by the cavitation degree within a nozzle. Every type of nucleation and flow regime inside a nozzle gives a different result in the breakup mechanism. A higher cavitation length induces a wider spray angle and can lead to finer droplets (Abderrezzak & Huang, 2016). Even though cavitation can enhance the atomization of fuel sprays, Wu et al. (2017) found that it degrades the spray stability and nozzle lifetime. It was also found that the subsequent explosion or implosion of the bubbles can accelerate the breakup mechanism of a liquid jet (Lefebvre & McDonell, 2017). However, cavitation may cause severe erosion inside a nozzle passage.

Sou et al. (2007; 2014) have investigated the relationship between Reynolds number and cavitation number while classifying four types of cavitation inside a nozzle. For both no cavitation and developing cavitation, the liquid jet took the form of a "wavy jet." Spray-like breakups only form during supercavitation. If a hydraulic flip occurs inside the nozzle, the breakup of the liquid jet takes the form of a flipping jet.

There are many studies about cavitation inside spray for combustion applications, either simulations or experimental approaches, and their effects on liquid jet atomization. (Andriotis et al. 2008) identified cavitation that occurred inside a nozzle of fuel injection used in automotive and marine diesel engines as the main parameter that will affect the momentum of the injected liquid, the nozzle coefficient of discharge, and the spray angle of the fuel injected into the combustion chamber. The cavitation that occurred inside an injection nozzle was found useful in atomization processes to produce finer droplets, as studied by Serras-Pereira *et al*. (2010) for gasoline, iso-octane and n-pentane as working fluids.

The cavitation inside a jet nozzle has been a topic of interest because of its effects on the nozzle's flow and the resulting spray. Most of the research has focused on flows with a constant orifice diameter. The present investigation seeks to understand the cavitation phenomenon of jet flow through the throat. The location of the throat was varied, and the size of the throat was designed so that the liquid pressure drops below the saturation pressure at the liquid temperature.

METHODOLOGY

Three jet nozzles with different geometrical specifications were fabricated using acrylic rod. Internal and external surfaces were polished for clarity in visualising internal flow and any possibility of a cavitation phenomenon (Abderrezzak & Huang, 2016; Andriotis et al. 2008; Wei et al. 2023). The schematic diagram and the dimensions of the nozzles are shown in Figure 1 and Table 1, respectively.

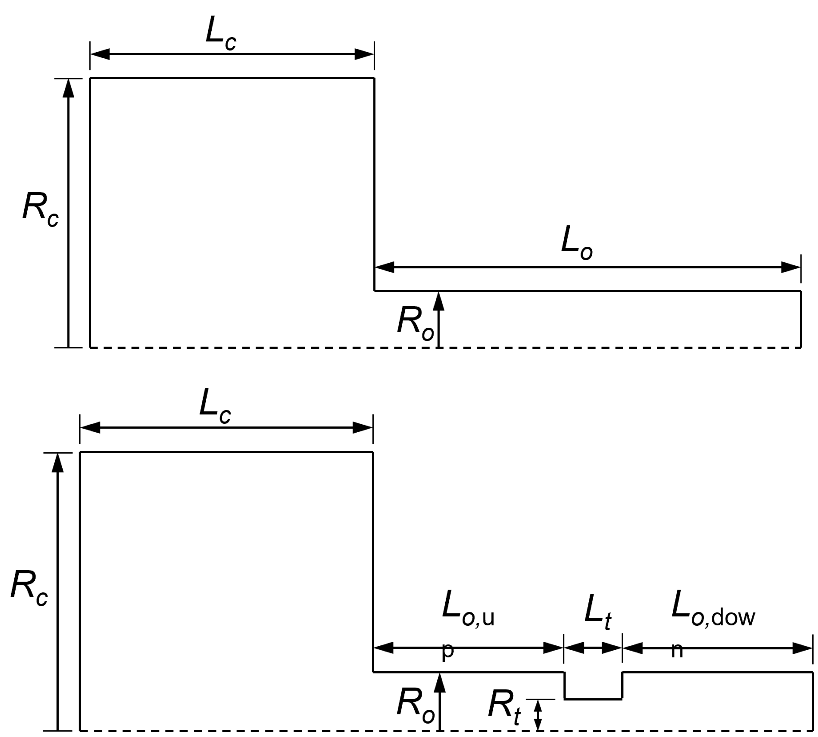

FIGURE 1. Schematic diagram of a) benchmark jet nozzle and b) jet nozzle with throat. Subscripts c, o and t represent chamber, orifice, and throat, respectively.

TABLE 1. Geometrical specifications of the jet nozzle, in mm

	Nozzle 1	Nozzle 2	Nozzle 3
R_c	15	15	15
R_o	2.5	2.5	2.5
R_t	N/A	1.5	1.5
L_c	40	40	40
L_o	30	N/A	N/A
$L_{o,\mathrm{up}}$	N/A	0	12.5
$L_{o,\mathrm{down}}$	N/A	25	12.5
L_t	N/A	5	5

All nozzles were tested using filtered water as the working fluid. The schematic diagram of the experimental setup is shown in Figure 2. A 16.2 megapixel digital camera with a 300mm focal length is used to capture images of the resulting sprays. The camera settings are shutter speed: 1/250, f-stop: f/5.6, and ISO: 100. Each nozzle was tested with injection pressures between 1 bar and 3 bar, with an increment of 0.5 bar. A shadowgraph technique is used to measure the spray parameters accurately and this method was applied by various group of researchers (Abderrezzak & Huang, 2016; Wei et al. 2023). The flash duration is set to approximately 26 microseconds to avoid motion blur while providing enough light for image processing.

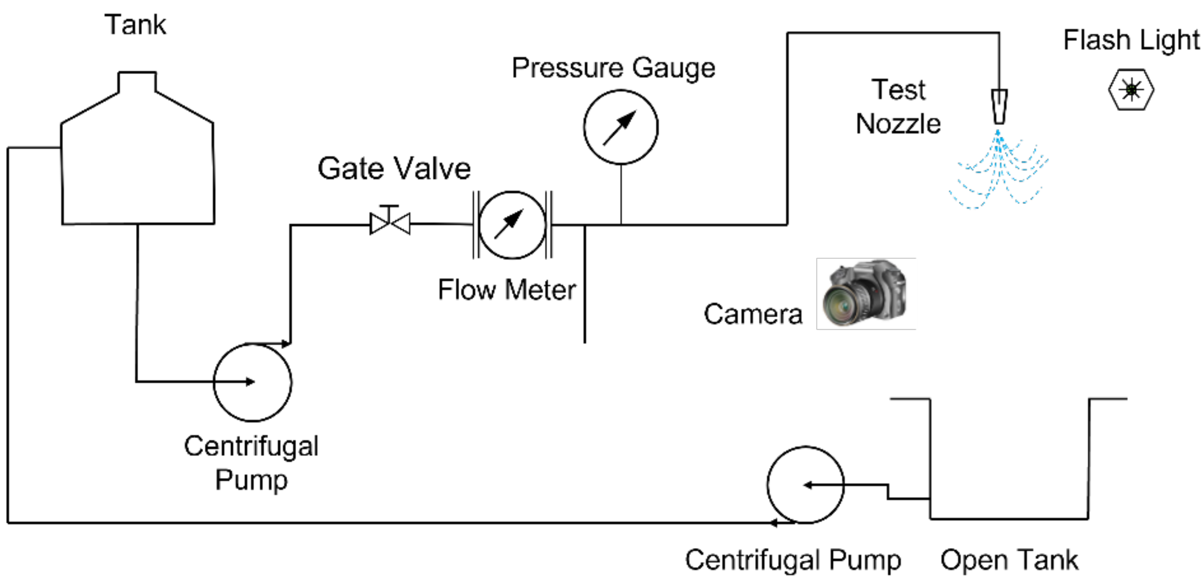

FIGURE 2. Schematic diagram of experimental setup.

RESULTS AND DISCUSSION

A total of three nozzles were tested with filtered liquid water at pressures ranging from 1 bar to 3 bar. Figure 3 shows the internal flow of Nozzle 1 at the exit orifice section. There is no cavitation observed at this injection pressure. This observation can be attributed to the fact that the liquid mean velocity in the exit orifice is not sufficiently large to produce a lower local pressure than the liquid's saturation pressure.

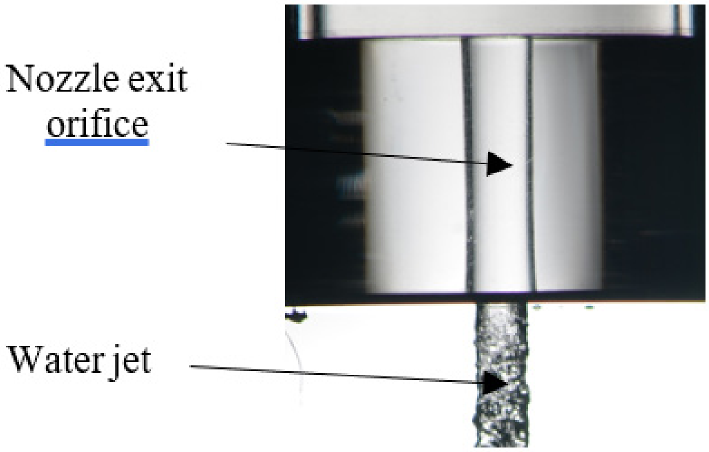

FIGURE 3. Internal flow of Nozzle 1 at injection pressure of 1 bar

The cavitation phenomenon is usually characterized by the cavitation number, defined by:

$$Ca = \frac{P_o - P_v}{\frac{1}{2}(\rho_l V^2)}, \tag{1}$$

where V is the liquid mean velocity, ρ is the liquid density, P_o is the atmospheric pressure, and P_v is vapor pressure. Cavitation number (C_a) is a dimensionless variable that is used to characterize the potential of the flow to cavitate. The cavitation number for Nozzle 1 at an injection pressure of 1 bar is 3.12. This value is much higher than the incipient cavitation number reported in the previous study, which is approximately 0.94 (Sou et al. 2007), hence the flow is less likely to cavitate. The experiment could not be continued at higher injection pressures as the exit orifice diameter is relatively large and the pump limit was reached.

Figure 4 shows the internal flow of Nozzles 2 and 3 at various pressures. At injection pressure of 1 bar, it was observed that cavitation appeared only near the inlet of the nozzle throat for Nozzle 2 (as shown in Figure 4(a)). This type of cavitation is classified as developing cavitation. When the injection pressure is increased to 1.5 bar, the cavitation extends to the part of the nozzle exit orifice. Secondary cavitation may be induced due to the sudden expansion further downstream. This type of cavitation is classified as mixed cavitation. A further increase in injection pressure (2 bar) extends the cavitation further downstream, but still in the mixed cavitation regime. The cavitation length increased from 2.25mm to 6.4mm and from 6.4mm to 10.8mm when the injection pressure increased from 1 bar to 1.5 bar and from 1.5 bar to 2 bar, respectively. At P_i = 2.5 bar, the cavitation extends to the exit plane. This type of cavitation is classified as supercavitation. It has been reported previously that supercavitation enhances liquid jet atomization (Sou, Tomiyama, Hosokawa, Nigorikawa, & Maeda 2006).

The effects of injection pressure (nondimensionalized to the vapor pressure) on the normalized cavitation length, L_{cav} (defined as the ratio of the streamwise length of the cavitation zone to the exit orifice length), are shown in Figure 5(a). It was noted from the figure that the cavitation grew almost linearly (with the coefficient of determination of 0.9997) with the injection pressure for injection pressures below which cavitation hasn't reached the supercavitation state. The incipient cavitation number is determined by first solving the linear equation:

$$L_{\mathbf{cav}} = 0.285\frac{P_i}{P_v} - 0.211 \tag{2}$$

for L_{cav} = 0, which yields P_i/P_v = 0.74. The incipient cavitation number is then predicted by substituting the value of P_i/P_v in the relation between the nondimensional injection pressure and the cavitation number shown in Figure 5(b). The approximate relation was obtained by curve fitting data in Figure 4(b) by power least squares regression, which yields:

Injection pressure, P_i (bar)	1	1.5	2	2.5	3

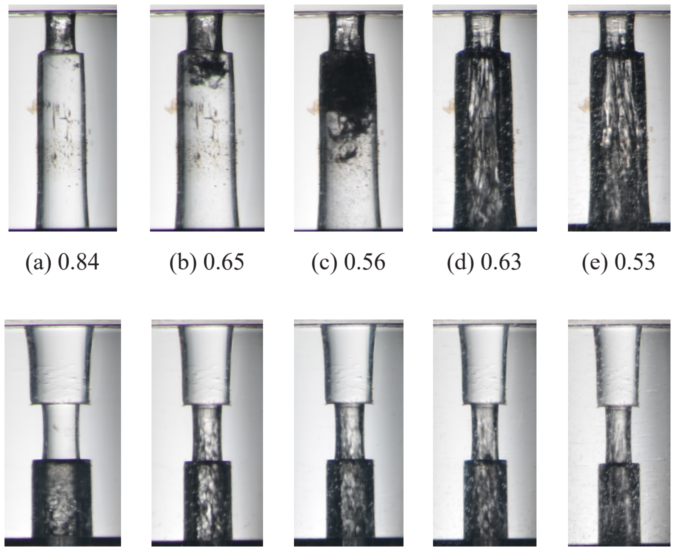

FIGURE 4. Internal flows of Nozzles 2 and 3 at various injection pressures and Cavitation numbers as indicated.

It is important to note that the choice of the least squares regression approach is arbitrary with the objective of a maximum coefficient of determination. The substitution yields the predicted incipient cavitation number of 9.65. This value is in the same order of magnitude as that reported in (Zhang et al. 2011) for the case of sudden expansion.

It is interesting to note that there is no cavitation at both edges of the sudden contraction at Nozzle 3 for an injection pressure of 1 bar. Still, cavitation appeared at the edge of sudden expansion, as shown in Figure 4(f). At higher injection pressures, however, cavitation begins at the inlet of the nozzle throat and extends to the nozzle exit orifice, as indicated in Figure 4(g-j). This is because the downstream length of the nozzle exit orifice of Nozzle 3 is shorter than Nozzle 2, and the flow doesn't have a sufficient distance to reattach to the wall.

Figure 6(a) shows the cavitation regime map for Nozzles 2 and 3. The Reynolds number was calculated based on the length and velocity, which are scaled with the exit orifice diameter and the mean flow velocity. Nozzle 1 is not included in the plot since the cavitation number is more significant than the other nozzles, i.e., 3.12. It can be seen from this figure that at a relatively large cavitation number, the cavitation regime transitioned from developing to mixed, and finally to supercavitation. However, for Nozzle 3, cavitation formed at the sudden expansion edge at a higher cavitation number. It is also noted that the flow inside Nozzle 3 achieved a supercavitation state at a relatively higher cavitation number since the length of the downstream exit orifice section is shorter than its Nozzle 2 counterparts. Furthermore, it is also interesting to note that for Nozzle 2, a supercavitation state was achieved at a cavitation number of 0.63, but returned to a mixed state at 0.56, and finally reached a supercavitation state again at 0.53. This observation deserves further attention; however, it is out of the present scope to discuss its reason.

Figure 6(b) plots the discharge coefficient against the cavitation number for Nozzles 2 and 3. In general, it can be seen that when the internal flow has reached a supercavitation state, the discharge coefficient is the lowest and is almost uninfluenced by the cavitation number. This observation is attributed to the fact that the flow was separated from the exit orifice wall, thus reducing the effective flow area. It was also noted that longer cavitation leads to a lower value of the discharge coefficient and that a case with no cavitation (i.e., Nozzle 1) has the highest discharge coefficient of 0.56.

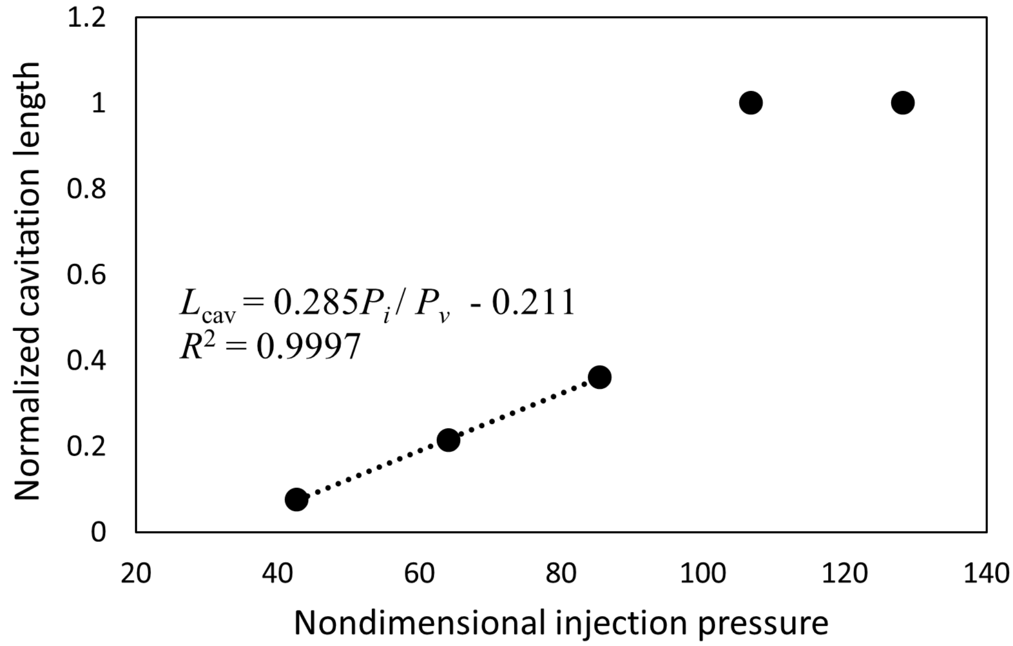

(a)

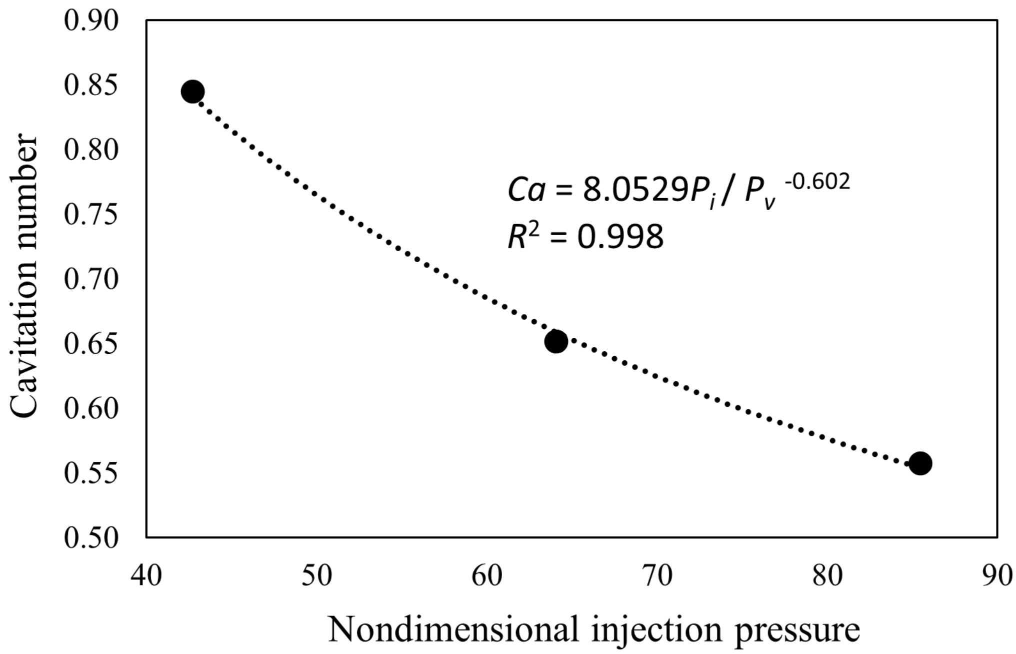

(a)

FIGURE 5(a). Growth of cavitation in the streamwise direction for various injection pressures for Nozzle 2. The dotted line represents curve fitted to the data by linear least squares regression and the dashed line represents the normalized length of the throat section and (b) nondimensional injection pressure plotted against cavitation number. The dotted line represents the curve fitted to the data by power least squares regression.

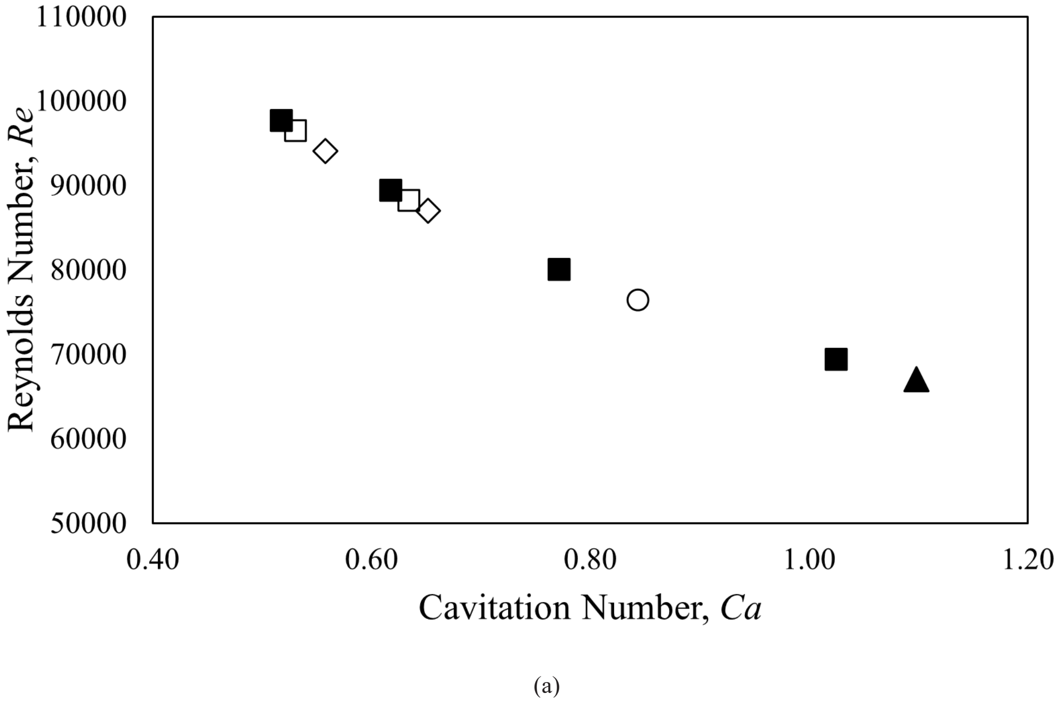

FIGURE 6 (a). Cavitation regime map and (b). Discharge coefficient plotted against Cavitation number for Nozzles 2 and 3. Hollow and solid symbols represent Nozzles 2 and 3, respectively. The circular, diamond, square and triangle symbols represent cavitation regimes of developing, mixed, super and sudden expansion, respectively.

CONCLUSION

Liquid jet flows with a cavitation phenomenon were experimentally investigated. The flows were visualized using the shadowgraph technique. Different cavitation regimes were classified, and the cavitation number's effect on the discharged coefficient was examined at various injection pressures. It can be concluded that a lower cavitation number leads to the onset of cavitation and that cavitation is more likely to occur at the edge of sudden expansion rather than sudden contraction. There were five cavitation regimes identified, and they depend on the cavitation number and the location of the throat. Furthermore, longer cavitation leads to a lower value of the discharge coefficient. In the limiting case of supercavitation, the discharge coefficient was reduced to a minimum and became less dependent on the cavitation number.

ACKNOWLEDGEMENT

This research was supported by the Ministry of Higher Education Malaysia through Fundamental Research Grant Scheme (FRGS), Grant No: FRGS/1/2019/TK03/UITM/02/14. This acknowledgment is also extended to Research Management Center (RMC) of UiTM.

DECLARATION OF COMPETING INTEREST

None

REFERENCES

Abderrezzak, B., & Huang, Y. 2016. A contribution to the understanding of cavitation effects on droplet formation through a quantitative observation on breakup of liquid jet. *International Journal of Hydrogen Energy* 41(35): 15821–15828.

Ali Othman, N. T., & Fahmi Mohd Razali, M. E. 2019. Drying of instant coffee in a spray dryer. *Jurnal Kejuruteraan* 31(2): 295–301.

Andriotis, A., Gavaises, M., & Arcoumanis, C. 2008. Vortex flow and cavitation in diesel injector nozzles. *Journal of Fluid Mechanics* 610: 195–215.

Daikoku, M., & Furudate, H. 2003. Effect of the cavitation in a nozzle on the liquid breakup. *Proceedings of ICLASS 2003, 9th International Conference on Liquid Atomization and Spray Systems*.

Etminan, A., & Harun, Z. 2021. Forced convective heat transfer analysis for two-dimensional slot jet of water-CuO Nanofluid. *Jurnal Kejuruteraan* 33(2): 229–238.

Lefebvre, A. H., & McDonell, V. G. 2017. *Atomization and Sprays*. 2nd edition. Boca Raton: CRC Press.

Li, D., Liu, S., Wei, Y., Liang, R., & Tang, Y. 2018. Numerical investigation on transient internal cavitating flow and spray characteristics in a single-hole diesel injector nozzle: A 3D method for cavitation-induced primary break-up. *Fuel* 233: 778–795.

Lü, M., Ning, Z., Yan, K., Fu, J., & Sun, C. 2015. Instability and breakup of cavitation bubbles within diesel drops. *Chinese Journal of Chemical Engineering* 23(1): 262–267.

Qiu, S., Xiao, D., Zhang, X., Wang, S., Wang, T., Li, X., & Xu, M. 2022. Experimental investigations of the phase change impacts on flash boiling spray propagations and impingements. *Fuel* 312: 122871.

Serras-Pereira, J., Van Romunde, Z., Aleiferis, P. G., Richardson, D., Wallace, S., & Cracknell, R. F. 2010. Cavitation, primary break-up and flash boiling of gasoline, iso-octane and n-pentane with a real-size optical direct-injection nozzle. *Fuel* 89(9): 2592–2607.

Sher, E., Bar-Kohany, T., & Rashkovan, A. 2008. Flash-boiling atomization. *Progress in Energy and Combustion Science* 34(4): 417–439.

Shervani-Tabar, M. T., Parsa, S., & Ghorbani, M. 2012. Numerical study on the effect of the cavitation phenomenon on the characteristics of fuel spray. *Mathematical and Computer Modelling* 56(5–6): 105–117.

Sou, A., Biçer, B., & Tomiyama, A. 2014. Numerical simulation of incipient cavitation flow in a nozzle of fuel injector. *Computers and Fluids* 103: 42–48.

Sou, A., Hosokawa, S., & Tomiyama, A. 2007. Effects of cavitation in a nozzle on liquid jet atomization. *International Journal of Heat and Mass Transfer* 50(17–18): 3575–3582.

Sou, A., Tomiyama, A., Hosokawa, S., Nigorikawa, S., & Maeda, T. 2006. Cavitation in a Two-Dimensional Nozzle and Liquid Jet Atomization (LDV Measurement of Liquid Velocity in a Nozzle). *JSME International Journal Series B* 49(4): 1253–1259.

Wang, Z., Dai, X., Liu, F., Li, Z., & Wu, H. 2018. Breakup of fuel sprays under cavitating and flash boiling conditions. *Applied Thermal Engineering* 143: 22–33.

Wei, Y., Zhang, H., Fan, L., Li, B., Leng, X., & He, Z. 2023. Experimental study on influence of pressure fluctuation and cavitation characteristics of nozzle internal flow on near field spray. *Fuel* 337.

Wu, S., Xu, M., Hung, D. L. S., & Pan, H. 2017. In-nozzle flow investigation of flash boiling fuel sprays. *Applied Thermal Engineering* 117: 644–651.

Zhang, J. M., Yang, Q., Wang, Y. R., Xu, W. L., & Chen, J. G. 2011. Experimental investigation of cavitation in a sudden expansion pipe. *Journal of Hydrodynamics* 23(3): 348–352.